Pergamon

PII: S0301-9322(96)00078-X

Int. J. Multiphase Flow Vol. 23, No. 3, pp. 409–424, 1997

Printed in Great Britain
0301-9322/97 $17.00 + 0.00

SLOW VISCOUS FLOWS OF HIGHLY CONCENTRATED SUSPENSIONS—PART I: LASER–DOPPLER VELOCIMETRY IN RECTANGULAR DUCTS

A. AVERBAKH, A. SHAULY, A. NIR and R. SEMIAT
Department of Chemical Engineering, Technion Institute of Technology, Haifa 32000, Israel

(Received 29 June 1995; in revised form 2 October 1996)

Abstract—A non-invasive experimental technique which enables optical penetration into the bulk of a flowing liquid–solid concentrated suspension was employed to study such flows. Matching of refractive indices of the continuous and dispersed phases was used to establish optimal conditions for the quality of the optical signals and can be used to measure concentration in the flowing dispersion. Laser–Doppler anemometry was applied to measure velocity profiles in a rectangular duct and to detect velocity fluctuations in the viscous flow of the concentrated suspension induced by the particles presence. The existence of a net drift of particles in a concentrated suspension is demonstrated. © 1997 Elsevier Science Ltd. All rights reserved.

Key Words: concentrated suspensions, laser–Doppler velocimetry, particles migration, viscous flow

1. INTRODUCTION

Concentrated solid–liquid dispersions exist in nature and in industrial processes. In nature, dispersion flows of similar type can be found for various biological suspensions such as body blood. In industry, many processes are involved with a slurry that is being mixed in a single vessel or is pumped from one point to another. In some cases, it is desired to transfer the slurry as a homogeneous mixture without allowing solid precipitation. On the other hand, when phase separation is needed, density differences are used to cause sedimentation. Such countercurrent motions take place in settlers, filters or centrifuges, while cocurrent slurries flows occur in crystallizers, solid–liquid mixers, reactors, pipes, etc. Understanding of the flow characteristics of dispersions is, thus, important for better design and control of such processes.

The flow of concentrated suspension is characterized by the strong interaction between neighboring particles. This interaction results in the now familiar shear induced migration phenomenon (Leighton and Acrivos 1987a,b). The migration of particles in the flowing suspension influences velocity and particle concentration distributions thereby affecting the characteristics of the flow to become different from that known for a homogeneous fluid or a suspension. Particle migration also exists in sedimentation flows where particles move in one direction while fluid is permeating in the opposite direction (Ham and Homsy 1988). This type of flow is affected by fluid and particle properties, and the separation is highly sensitive to fluctuations in particle motion which appear to be of the same order of magnitude as the net motion. The nature of this countercurrent flow, needs further investigation to better understand the microscopic motion involved and the resulting particle migration.

To study shear induced particle migration, local information is needed at different positions in the flow. Velocity fluctuations, local particle concentration and the effect on the local suspension viscosity are needed for full comprehension of the phenomena involved. Invasive measurement methods as physical sampling or the use of hot wire anemometers and other types of velocity probes, interfere with the flow and distort the results. It is necessary to obtain the needed information by using non-invasive methods, which usually involve different types of radiation penetrating the measured system. Leighton and Acrivos (1987b), observed the motion of marked particles in a Couette flow device to measure particles diffusion. Phillips *et al.* (1992) employed a Nuclear Magnetic Resonance imaging technique in a similar flow device to detect local changes of concentrations induced by particles migration. Abbott *et al.* (1993) summarize different

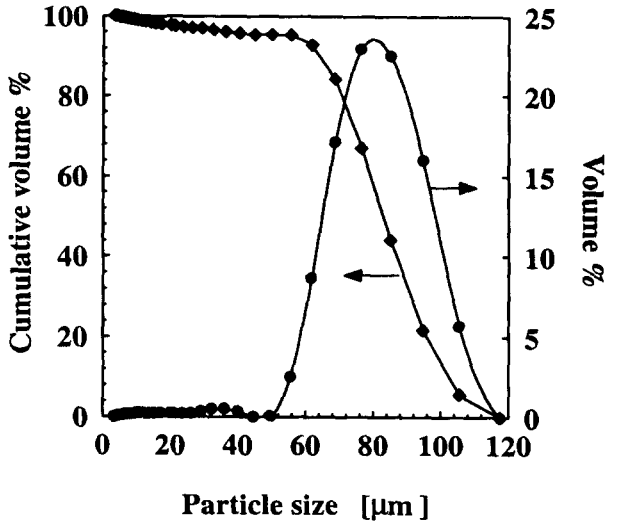

Figure 1. Differential and cumulative particle size distributions.

non-invasive measurement methods, including the use of X-ray device to track falling balls during effective viscosity measurements in suspension. The laser grating anemometry method (Semiat and Dukler 1981) is particularly suitable to detect the motion of large transparent solid particles, droplets and bubbles. A new technique, Laser Induced Photochemical Anemometry (LIPA) was presented recently by Falco and Nocera (1993) and was used to measure local velocities in dense liquid–solid flows.

Among the different experimental methods for the investigation of fluid flows known today one of the most popular methods, that has wide possibilities and applications, is the method of Laser–Doppler Anemometry (LDA) (Durst *et al.* 1976; Drain 1980). The significant advantage of this non-invasive method is its high resolution without influencing the flow. It gives a high accuracy and the possibility to measure true and unaffected main flow parameters. The LDA method was conceived in the early 1960s. Since that time LDA became a reliable flow measuring method and considerable progress has been achieved in LDA hardware and in understanding the fundamental properties of LDA signals (Drain, 1980).

Laser–Doppler Velocimetry (LDV) is based on light beams that intersect at the measurement point inside the flow cell. This method is frequently used for velocity measurement in homogeneous

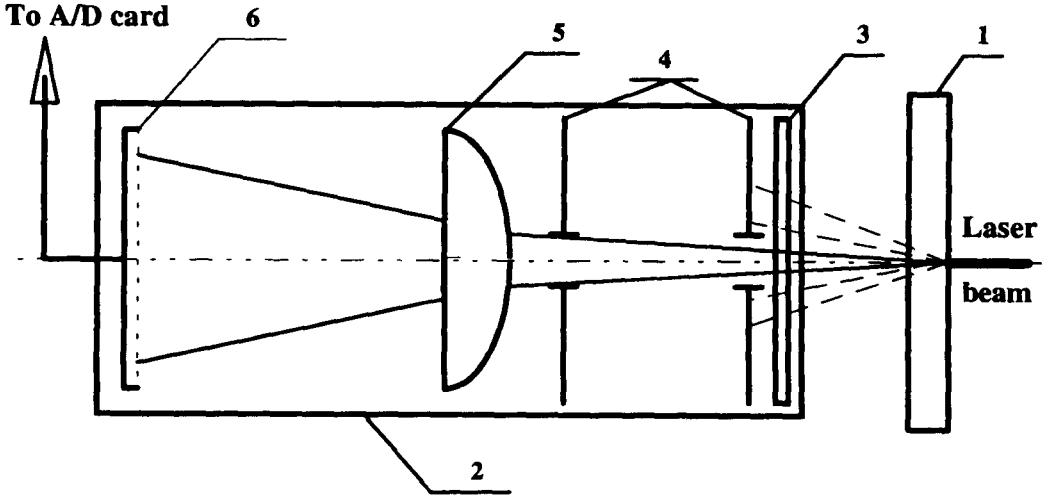

Figure 2. A schematic description of the optical unit used for the measurement and control of the particle–fluid matching refractive index. (1) cavity; (2) optical unit; (3) neutral filter with variable optical density; (4) apertures; (5) cylindrical lens; (6) bench of photoreceivers.

transparent flow systems. When suspensions are to be considered, the ability to use this method is diminished by the ability of the light beams to penetrate into the bulk of the flow, and by the dispersion of the light due to scattering from multiple particle surfaces. Consequently, velocity measurements are restricted to regions adjacent to the flow system's transparent walls. These problems and the resulting restrictions intensify with the increase of particle concentration and inhibit measurements of data in the bulk. A method to overcome this inhibition relies on the ability to match the refractive indices of the fluid and the particles at the laser beam wavelength, thereby rendering the suspension transparent to the beam and minimizing the light dispersion due to scattering. In the absence of such matching, particle volume concentration of more than several percent results in multiparticle scattering (Ischimaru 1978), an effect that leads to noisy optical signals and ultimately to a complete loss of information. There have been several works that proposed and developed the application of LDA in multiphase flows using refractive index matching approach. Zisselmer and Molerus (1979) reported application in turbulent flow with particles volume concentration up to 0.056. Nouri *et al.* (1986, 1988) measured particle velocities in pipe turbulent flow. Park *et al.* (1989a,b, 1992) also measured velocities of 2 μm particles slurries in laminar and turbulent flows. In all the studies mentioned above the particle volume fractions were under 0.14, a rather limited particle concentration.

It is well known (Hulst 1957) that the energy dispersed from a spherical particle is proportional to $(n' - 1)^2$, where n' is the ratio of the particle to fluid refractive indices. In the case of a suspension with a high particle concentration, scattering from interface is influenced by particles refractive index variation. There is a strong dependence of the scattering in a cloud of particles on the distribution of n' and this dependence increases steeply with the increase of particles concentration. Recent works report the application of careful refractive index matching techniques to study of flows of suspensions with considerably higher particles concentration. Abbas and Crowe (1987) studied flow properties of slurries in tubes and Koh *et al.* (1994) used LDA to detect velocities and particle concentration distribution of slow viscous suspension flow in a rectangular duct. In these works the particle volume concentration was limited to 0.3.

The absence of LDV experimental data in suspensions with high particle concentration reflect the difficulties involved in obtaining such results. Yet the interesting microscopic phenomena such as particle migration are pronounced in these high concentrations. There is a need for application of the non invasive measurement method beyond the existing previous limited volume concentration of 0.3.

This work presents the use of LDV in velocity measurements of flowing concentrated suspensions. A successful application of LDV in the bulk of the flowing suspension was achieved with particle volume fraction up to 0.5. In section 2 we describe an on-line technique used to obtain optimal refractive index matching adjustment and control. This matching adjustment procedure enables on line measurements of average concentration along the laser beam. The application of LDV to obtain velocity and velocity fluctuations is described in section 3 where the ability to demonstrate and measure local particle drift across streamlines in the creeping flows of concentrated suspensions is also demonstrated.

2. EXPERIMENTAL SYSTEM AND PROCEDURES

The limitations described earlier impose severe constrains on the experimental system design. The choice of particles and fluid with controllable refractive indices is the first step to consider and will be reported below. Three systems are described herewith: Optical optimization system for the process of matching refractive indices, which may also be used for particle concentration measurements, the flow system and the laser–Doppler system for the measurement of velocities and velocity fluctuations.

2.1. Suspension components

Particles. The choice of particles for the make of the suspension for these experiments must satisfy several conditions: The fluids and particles must be chemically inert, the fluid must not dissolve, swell or soften the particles and the particles must have uniform physical properties, particularly the density and the refractive index.

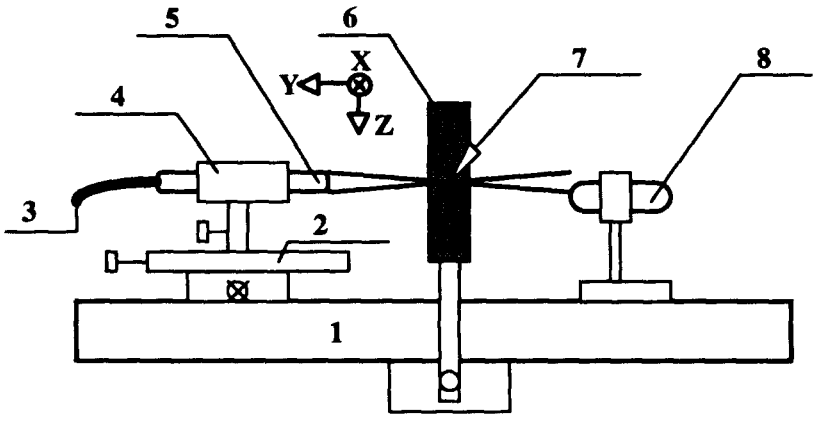

Figure 3. Experimental set-up for refractive index matching and for laser–Doppler anemometry. (1) Optical bench; (2) 2D table; (3) optical fiber transmitting laser beams; (4) probe mounting; (5) probe; (6) cavity or flow duct; (7) probe volume; (8) refractive index measurement unit.

In this investigation spherical PMMA (polymethylmetacrylate) particles were used. The spheres were 85 $\pm$ 15 μm in diameter and size distributions of a sample are given in figure 1. The density of the particles was measured by suspending the particles in a set of test tubes with a solution of NaCl of various concentrations. This procedure was used mainly to eliminate from the experiments the fraction of particles containing bubbles. The particles refractive index was measured by means of minimization of light scattering from a suspension when the refractive index of the liquid component was monotonically changed. At 28°C particle density was found to be 1.175 g/cm^3 and their refractive index was 1.491 for a wavelength of 589.3 nm.

Fluid. The fluid phase of the suspension must also satisfy several requirements. First, the ability to match the refractive indices of the suspension phases is essential. Second, the matching of the density of the suspension phases is also necessary to minimize particle drift, relative to the fluid, caused by density differences. Third, since the effective viscosity of a suspension with a high particle volume concentration can be orders of magnitude higher than the viscosity of the suspending fluid, the ability to have a viscosity modification of the liquid component is advantageous. Apart from the above mentioned requirements any chemical interaction between particles and liquid has to be absent.

Three fluids were selected, similar to the components of the mixture used by Milliken *et al.* (1989) and Abbott *et al.* (1993). Triton X-100 (density 1.055 g/cm^3, refractive index 1.4866, viscosity 280 cp at 28°C), Ucon Oil H-450 (density 1.084 g/cm^3, refractive index 1.4571, viscosity 120 cp) and Tetrabromoethane (TBE) (density 2.943 g/cm^3, refractive index 1.6238, viscosity 1 cp). An appropriate mixture of these fluids satisfies the requirements specified above and is, therefore, suitable as the liquid phase of the suspension. Tinuvin 328 (a product of Ciba–Geigy Corp.) is also added to the mixture (0.3% of the TBE Weight) in order to reduce ultraviolet degradation of the TBE. In the case of a dilute suspension there is a possibility to increase the viscosity of the liquid mixture by replacing the Ucon Oil H-450 with Ucon H-1,400 or Ucon Oil H-90,000. The densities and refractive indices of these oils are similar, but the viscosities are significantly different. The fraction of each component in a mixture having a refractive index of PMMA (1.4910) depends strongly on temperature.

Suspension. The suspension was prepared by mixing the particles and the fluid for a few hours to obtain a homogeneity. The mixture was held under high vacuum for a few days to ensure the removal of dissolved air and any entrapped bubbles. The pouring of the suspension into the flow system was done carefully to avoid entrainment of undesired air. The careful removal of the air helps in three ways. It eliminates false velocity signals due to bubble motion, it minimizes the appearance of liquid–gas–solid interfaces in the laser beam path and it prevents possible cavitation in the circulating pump.

2.2. Refractive index matching system

Refractive index measurements were carried out by means of a Bausch and Lomb refractometer. This instrument measures the refractive index for the yellow line of mercury (line D, 589.3 nm). During the experiments Argon (blue–green) Laser was used and it was found necessary to recalculate the refractive values for the different wavelengths.

The corrected refractive index for the green laser (n_G) having a wavelength λ_G, was obtained from the measured value n_D using the interpolation

$$n_G = n_D + \frac{\lambda_G - \lambda_D}{\lambda_R - \lambda_B}(n_R - n_B), \qquad [1]$$

where the symbols R and B denote the red and blue lines in the spectrum of hydrogen, respectively (486.1 and 656.3 nm).

The optical unit for the measurement of the particles refractive index and the control of the refractive index matching is presented in figure 2. The laser beam crosses a cavity (1) which contains a mixed suspension of known particle concentration. Light scattered by the particles passes a neutral optical filter (3), two apertures (4) and a cylindrical lens (5) and falls on the bench of photoreceivers (6). The neutral filter (3) with variable optical density is needed because, even for a perfect refractive index matching, the intensity of light which passes the cavity changes significantly with particle concentration. The apertures (4) select only the central scattered light, which contains information about the refractive index matching, and cuts off peripheral light noise. The cylindrical lens (5) extends the passed light to a light sheet conforming to the geometry of the set of photoreceivers to increase the sensitivity of light distribution measurements. The bench (6) consisted of a set of 35 photodiodes with working dimensions of 4.4 × 0.9 mm, separated from each other by a gap of 0.1 mm. Thirteen photodiodes of the set were used. The electrical signals from the photodiodes are directed to an electronic unit with 13 channels which amplify the photodiode

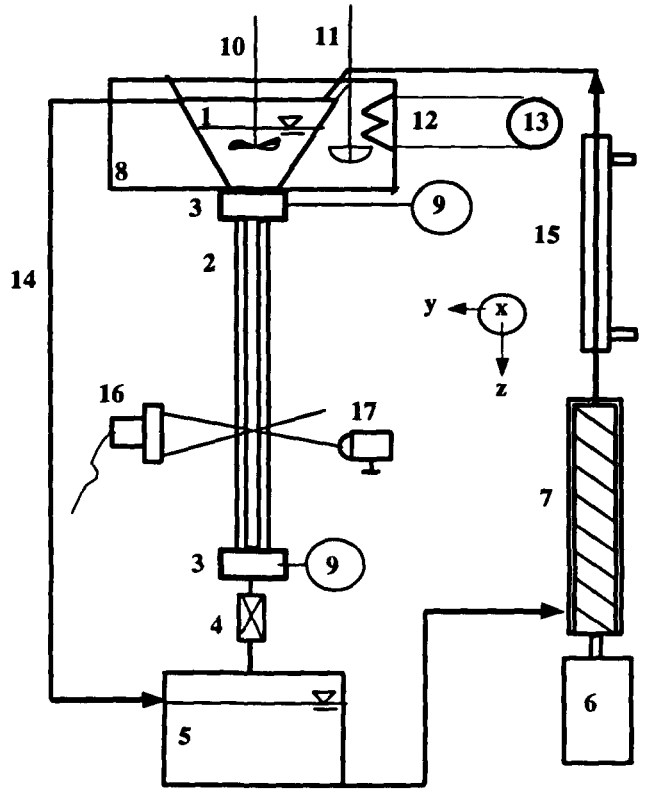

Figure 4. Flow system. (1) upper vessel; (2) duct; (3) connectors; (4) valve; (5) receiving vessel; (6) direct current motor; (7) screw pump; (8) water bath; (9) thermocouples; (10), (11) mixers; (12) heater; (13) heat control system; (14) bypass line; (15) heat exchanger; (16) fiber flow probe; (17) refractive index match measurement unit.

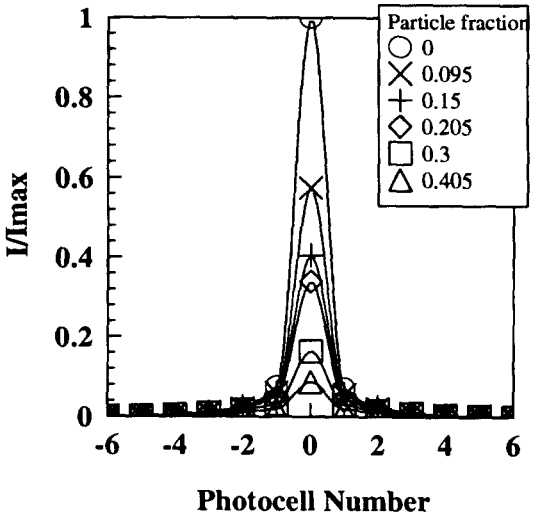

Figure 5. Normalized light intensity distributions of a laser beam that have passed the cavity filled with suspensions of various particle concentrations with minimum refractive index difference. I_{max} is the light intensity detected on the central photocell at zero particle concentration.

signals and send them to a data acquisition card (Flash-12, a product of Strawberry Tree Inc.), which was installed in a PC-486. A commercial software program was used (Workbench, a product of Strawberry Tree Inc.). This software incorporated a multiplexor which samples all channels of the electronic unit sequentially and displays the distribution curve of light intensity on the computer screen in real time. The acquired data were stored on a hard disk.

The measurement of particle refractive index was carried out by placing a suspension of PMMA particles in the fluid mixture into a small cavity with a cross section of 8 × 15 mm. To guarantee particle concentration homogeneity the suspension was continuously mixed by means of a magnetic stirrer. The refractive index of the liquid phase was monotonically changed resulting in a change of the shape distribution of the detected scattered light intensity. At the matching point the shape distribution of the scattered light intensity is the sharpest. At this point the refractive index of the liquid was measured by a refractometer. There are two ways to change the refractive index difference between the particles and the liquid. One way is a change in the relative components concentration of the solution by adding a component. The second way is by changing the suspension temperature since the temperature dependence of the liquid refractive index is much stronger than that of the solid (Ioffe 1974). The experiments showed identity of both methods near the matching point.

The same procedure was used to control the refractive index matching during a flow experiment. In this case the control was carried out by maintaining the temperature that gives the most narrow intensity distribution of the light that passed the flow cell described below. The optical cell described above was replaced by a rectangular duct placed in the flow system along the path of one of the laser beams used by the LDA, as explained below. Figure 3 shows schematically the relative position of the optical cell with respect to the flow system. In principle this method can also be used to measure the concentration of a suspension averaged along the path of a laser beam as is discussed in section 3.

The temperature was kept within an interval of $\pm 0.1^{\circ}C$ during velocity measurements. The working temperature was determined as the temperature of the suspension that gives the sharpest scattered light curve.

2.3. Flow system

The velocity measurements were conducted in a rectangular duct through which a steady flow of the suspension was maintained. A description of the arrangement is depicted in figure 4.

The system operated as follows: The upper vessel (1), in which the suspension was continuously mixed, was made of PMMA plates and has the shape of a truncated inverted pyramid. The

suspension flows from the vessel to a rectangular flow duct (2) and from there to the receiving vessel (5) through connectors (3). The connectors were also made of PMMA plates and provide a smooth transition between the flow cell and the adjacent sections. The flow cell was made of optical glass plates with parallel surfaces. The plates thickness was 4 mm and the distance between them is 8 mm. The channel in the flow duct has the form of a parallelepiped with a length of 380 mm and a cross section of 8 × 50 mm. The valve (4) placed between the flow cell (2) and the receiving vessel (5) controlled the suspension flow rate. The suspension was pumped to the upper vessel (1) by means of a screw pump (7) which was driven by a direct current motor (6) controlled by a variable power supply. This pump does not crash the suspension particles and provides a steady pressure without pulses or cavitation. Steady suspension flow rates in the flow cell were obtained using a bypass line (14). Since it was necessary to maintain the suspension temperature in the measured volume in a very narrow range to maintain a minimal liquid–solid refractive index difference, the temperature was kept within an interval of $\pm 0.1°C$ using the water bath (8) surrounding the upper vessel (1), a heat exchanger (15) located between the pump and the upper vessel and an electric heating ribbon placed on the flow cell (not shown in figure 4). The temperatures at the flow cell entrance and exit were measured by accurately calibrated thermocouples (9).

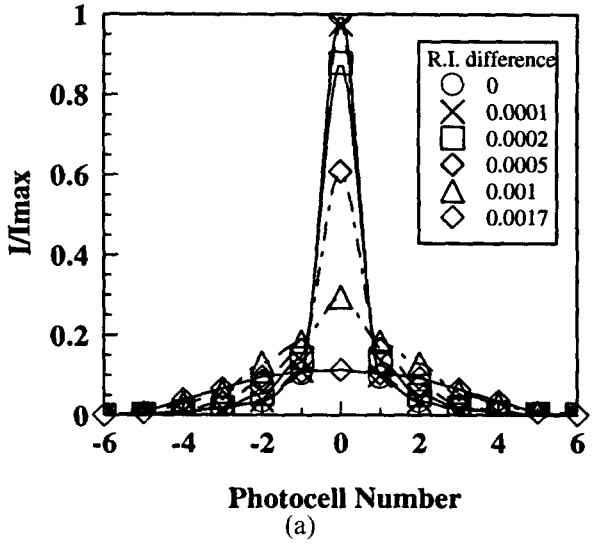

(a)

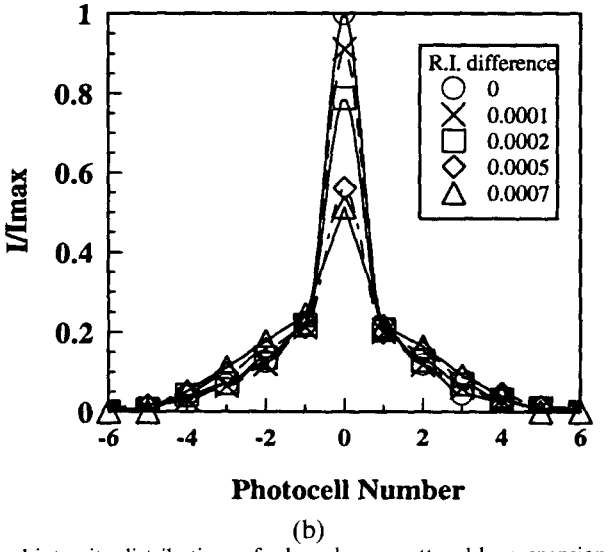

(b)

Figure 6. Normalized intensity distributions of a laser beam scattered by suspensions with fixed particle concentration at various refractive index differences between the particles and the liquid. (a) $\phi = 0.095$; (b) $\phi = 0.403$.

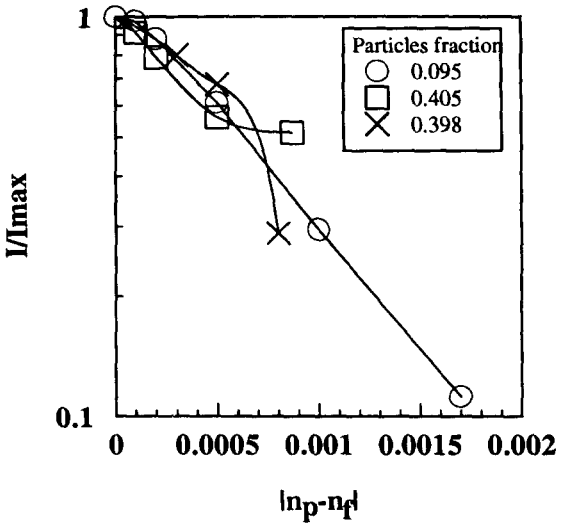

Figure 7. Normalized light intensity detected by the central photoreceiver of a laser beam scattered by suspensions with various concentrations vs refractive index difference between the particles and the fluid.

The vibrations of the flow cell were minimized by mounting the upper vessel, the flow cell and the connectors on a rigid frame. All optical components and the above mentioned frame were mounted on a massive optical bench placed on a table with legs cushioned with soft rubber segments. Air dampers preventing transmission of vibrations from the laboratory floor were placed between the bench and the table. A long strong pole was adjusted between the floor and the ceiling near the table with soft rubber at its edges. The receiving vessel, the mixer motor and the connecting tubes were supported by the pole. The connecting tubes were made of soft silicon material that extinguishes vibrations. Mixers were connected to their motors by means of long soft rubber tubes. All these precautions reduced vibrations down to values that were much smaller than the minimal root mean square (RMS) velocities of the suspensions.

2.4. *Laser–Doppler system*

A Dantec Laser–Doppler Anemometer (LDA) was used to measure the velocity. A 1 W Argon laser was employed (model Enterprise 610, by Coherent). The optical part of the system is the FiberFlow unit which consists of a series of fiber optical elements and lenses. It directs the beams to the target and collects the signals in a backscatter mode. The system also provides frequency shift and color separation. The Dantec system frequency shifter allows detection of negative and positive velocities which appear in measurements of fluctuations perpendicular to the main flow direction. A lens collects the back scattered light and a receiving fiber transmits the signals to a photomultiplier. The lens used has a focal length of 113 mm. The beam separation is 38 mm. It gives a half angle, θ, between the beams of 9.65°. The laser beam diameter on the focal lens is 2.2 mm. The used wave length of the laser beam is 514.5 nm. These parameters give an ellipsoidal measurement volume in air, henceforth referred to as the probe volume, with the following dimensions: $d_e \approx 34\ \mu m$, $d_e/\cos\theta \approx 34.5\ \mu m$, $d_e/\sin\theta \approx 202\ \mu m$ with d_e being the effective Gaussian diameter of the beam at the probe volume intersection location. The spacing distance between fringes in the probe volume is 1.55 μm. Figure 3 shows schematically the location of the FiberFlow probe with respect to the flow cell, and the path of the two laser beams in a vertical velocity measurement mode. At each point, 2000 Doppler signals were collected. The averaged velocity and the standard deviations of the 2000 velocity values were calculated.

The signals were processed by a computer controlled Dantec Burst Spectrum Analyzer (BSA) operated in continuous mode. Measurements results transfer and the parameters setup were performed from a host PC-486 computer via an IEEE-488 interface.

A software package provided by Dantec (Burstware) was used to perform the BSA control, data acquisition, data processing. Burstware also performs statistical analysis of the data obtained at a single position.

3. RESULTS AND DISCUSSION

3.1. Light intensity distribution in concentrated dispersion

Typical normalized intensity distributions of a green laser beam that have passed the cavity with suspensions of different volume fractions are presented in figure 5. The data were obtained by using the system described in figure 3. The abscissa denotes the position number of photoreceivers with the central one marked by 0. Presented on the ordinate are the scattered light intensities, normalized by the light intensity of the central photocell for a suspension with zero particle concentration (I_{max}). The data points were taken in suspensions at a temperature in which the refractive index difference $|\Delta n|$, was carefully reduced to the best achievable minimum. The effect of a finite non-zero refractive index difference between the fluid and the solid phases was studied for various particle concentrations. Several curves which correspond to refractive index differences for dispersions with particle volume fractions of 0.095 and 0.405 are depicted in figure 6(a) and (b), respectively. The refractive index difference was calculated from temperature measurements during the experiment. The sensitivity to the refractive index difference is well documented. It increases with the increase of dispersion concentration. The near Gaussian curves attain a sharper shape with the decrease of $|\Delta n|$.

When a laser light beam passes through a suspension, for which matching of the refractive indices of the phases was established, it is expected that the intensity will decay along the path of the beam. This decay results from the imperfect matching of the refractive indices due to minute deviation in temperature and to variations in material properties (especially in solids). The amount of scattering will thus depend on the curvature and the number of interfaces that the light beam crosses in its path. These reflect the cumulative effect of particle size distribution and their concentration in the suspension. This expected behavior is found in our experiments and is depicted in figure 7, where the intensity measured at the center photoreceiver, relative to the one with zero particle concentration, is displayed as a function of the refractive index difference. The relative light intensity clearly decays exponentially with the increase of the magnitude of the refractive index difference, $|\Delta n|$. Figure 7 also indicates the accuracy at which the refractive index difference could be established in order to permit a sufficient light intensity at the probe volume for meaningful anemometry response. Evidently the tolerated refractive index difference can be extended considerably for lower concentrations as seen in the curve corresponding to the concentration $\phi = 0.095$. At higher concentration, in our system, $|\Delta n|$ must be maintained below 0.0005.

The dependence of the relative intensity on suspension concentration is shown in figure 8. These data are taken as the reading at the central photodetector in figure 5 and correspond to the best

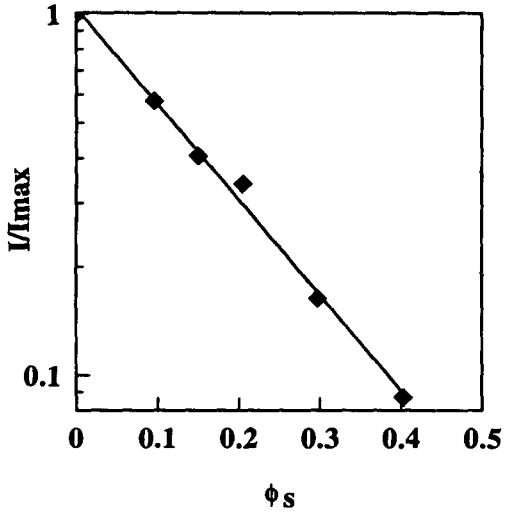

Figure 8. Normalized light intensity of a laser beam scattered by optically matched suspensions collected at the central photocell vs particle concentration. I_{max} is light intensity at the central photocell for suspension zero particle concentration.

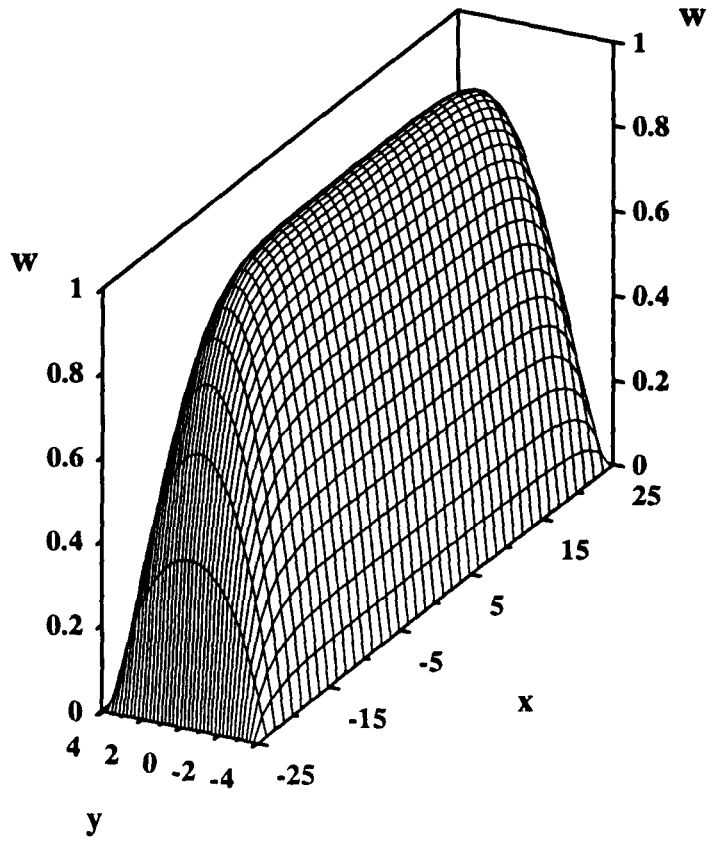

Figure 9. Velocity profile of a viscous homogeneous Newtonian fluid in a rectangular duct.

achievable refractive index matching in the system. A simple exponential decay of intensity with the increase of particle concentration was obtained. It should be noted that the decay corresponding to imperfect matching of refractive indices and to the increase of particle concentration, which enhance the amount of scattering of light passing through the suspension, becomes dominant over the natural decay due to light absorption typical to a homogeneous phase. If the relative intensity of a beam passing through a homogeneous sample is reduced by an extinction factor $e^{-\tau}$, where $\tau = ml$ is the usual optical depth of a sample along the light path l, in a heterogeneous suspension t should be modified to include the effects of $|\Delta n|$ on the average particle concentration ϕ_s. Figures 7 and 8 suggest that for a small $|\Delta n|$, τ may be presented in an effective form

$$\tau = m(1 + \alpha|\Delta n| + \beta\phi_s)l \qquad [2]$$

with α and β derived from the figures slopes, and is thus increased considerably to reflect the full complexities of multiple scattering in the concentrated suspension (Hulst 1957).

Figure 8 also suggests an on line method for the measurement of the particle volume fraction in the concentrated flowing suspensions. Naturally, these measurements should be carefully calibrated and would present an average concentration along the path of the laser light beam in the measurement cell.

3.2. *Velocity measurements in a unidirectional flow*

The velocity measurements were conducted in a duct with a rectangular cross section having a wide dimension of 50 mm ($-25 < x < 25$) and a narrow width of 8 mm ($-4 < y < 4$). The location of the measurement was $z = 295$ mm from the origin at the entrance to the flow cell. The homogeneous suspensions entering the flow duct are assumed Newtonian fluids with an effective viscosity given by (Krieger 1972)

$$\mu = \mu_0(1 - \frac{\phi}{\phi_m})^{-1.82}. \quad [3]$$

Here μ_0 is the viscosity of the suspending liquid and ϕ and ϕ_m denote the particles volume concentration and its maximum possible value, assumed $\phi_m = 0.6$, respectively. Following Schlichting (1965), the distance required to obtain a fully developed form of an inlet flow at the entrance region of a straight channel of width $2b$ is

$$z_b = \frac{\rho b^2 v_{av}}{3\mu} \quad [4]$$

where ρ is the suspension density and v_{av} denotes the average velocity. It follows that for the velocity measured in our experiments the distance z_b for the concentrated suspensions is typically less than 1 mm. It can thus be assumed that at any location along the flow cell, with its local particle concentration distribution, the unidirectional velocity profile is fully developed and is particularly so at the location of the measurement with the LDV, i.e. at $z = 295$ mm.

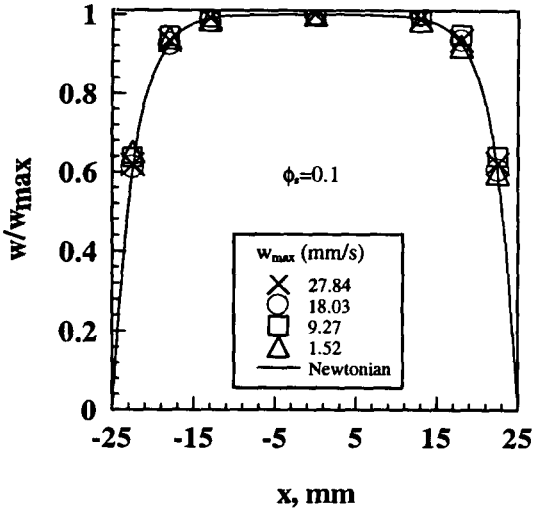

(a)

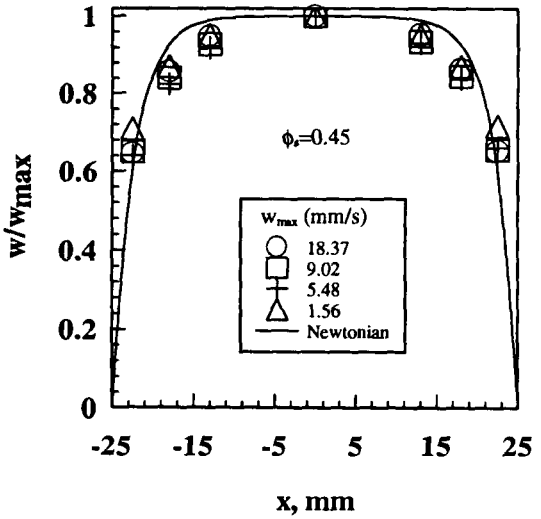

(b)

Figure 10. Vertical velocity measured at the symmetry plane $y = 0$ for a suspension with particle concentration. (a) $\phi_s = 0.1$; (b) $\phi_s = 0.45$.

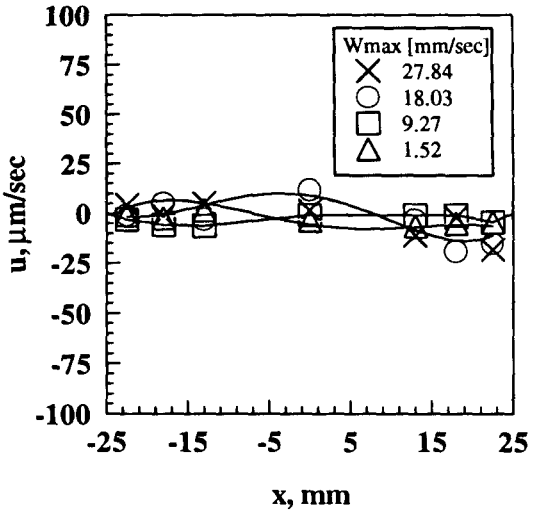

(a)

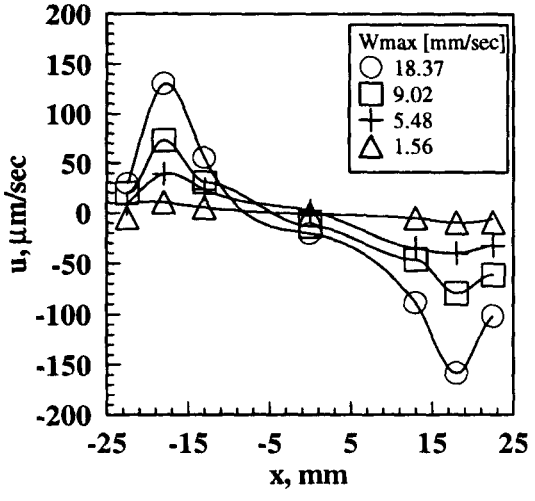

(b)

Figure 11. Horizontal velocity measured at the symmetry plane $y = 0$ for a suspension with particle concentration. (a) $\phi_s = 0.1$; (b) ϕ_s-0.45.

The velocity profiles for a fully developed incompressible viscous flow of a Newtonian fluid in this geometry can be obtained from the Stokes equations of motion, where the velocity and the gradient of the pressure are assumed unidirectional. These profiles, normalized by the maximum velocity w_{max} at the center of the flow cell, were obtained using a standard numerical procedure and are depicted in figure 9. The flat profile in the wider direction of the duct cross section and the almost parabolic profiles in the narrower direction are clearly evident.

Figure 10(a) shows vertical velocity profiles measured along the line $y = 0$ for a suspension with $\phi_s = 0.1$ normalized by the various values of the maximum velocity, w_{max}. All normalized velocities collapse onto one curve. The solid curve corresponds to the calculated Newtonian velocity at the middle plane (figure 9). The velocity profile at the measurement location, for all suspension flow rates, was clearly found identical to the one expected for a homogeneous Newtonian fluid.

Vertical velocity profiles corresponding to a concentrated suspension with $\phi_s = 0.45$ are depicted in figure 10(b). These profiles do not resemble the profiles for $\phi_s = 0.1$. They are curved rather than flat along the center portion. This behavior is similar, but not identical, for all given w_{max}. The profiles deviate from the calculated for a Newtonian fluid which is illustrated by the solid curve.

Although, due to the absence of entrance effects, the flow is expected to be unidirectional, we have also measured at each point the horizontal velocity. In figure 11(a) we show the measured horizontal velocity components for $\phi_s = 0.1$. At all measurement locations the horizontal velocity was found less than 20 μm/s, i.e. almost as the experimental accuracy. For the suspension with $\phi_s = 0.45$ the horizontal velocity measurements are depicted in figure 11(b). The horizontal velocity profiles are distinctly different from those obtained for the less concentrated suspension. It is readily seen that net horizontal velocities prevail and are directed from the side walls at $x = \pm 25$ mm toward the center at $x = 0$. It is also evident that these velocities increase in magnitude as the maximum vertical velocities increase. Since the fully developed vertical velocity profile for this suspension is almost instantaneously established it is concluded that the measured horizontal velocity indicate the existence of a net particulate drift from the side walls to the center. While this drift is almost undetectable for $\phi_s = 0.1$, it is clearly pronounced for $\phi_s = 0.45$. Apparently, it is significant enough to influence the vertical velocity profiles and promote deviations from the Newtonian curve as was evident in figure 10(b). For $\phi_s = 0.1$, where the horizontal drift was negligible, such deviations were not found. A comprehensive experimental study and a calculated model describing this phenomenon for various suspension concentrations is described in a following report (Shauly *et al.* 1997) henceforth referred to as Part II.

Figure 12 shows the standard deviation measured for the vertical and the horizontal velocity measurement for various suspensions concentrations and flow rates. Each point corresponds to the average of the STDs obtained at the three central measurement points of each curve in figures 10 and 11 and the data described in Part II. The magnitude of the standard deviations, particularly of these associated with the horizontal velocity components, and the dependence of the STD on the flow intensity and on the suspension particle concentration deserve a special attention. Since the standard deviation is considerably larger than the magnitude of the horizontal velocity it follows that many of the detected horizontal velocities have opposite components equal in magnitude which cancel each other in the averaging process. These are measured opposite components which are produced by the motion and the rotation of particles in the sheared

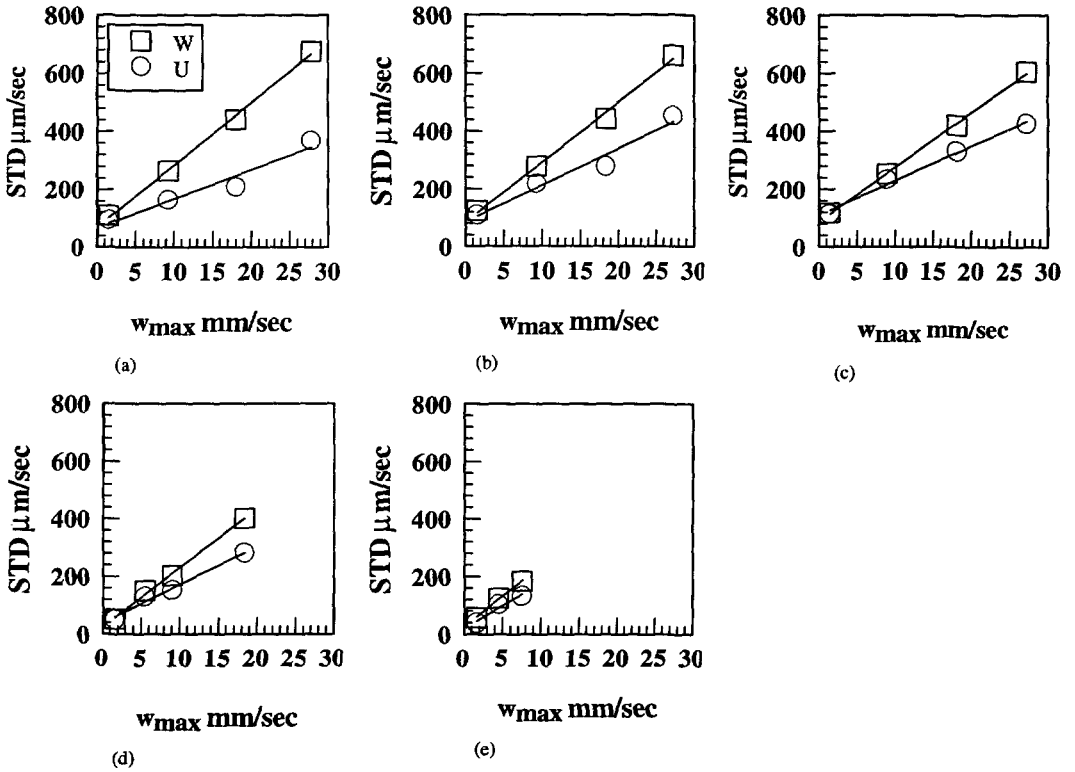

Figure 12. The dependence of the standard deviation of the magnitude of shear expressed in terms of w_{max}. □, Vertical STD; ○, horizontal STD. (a) $\phi_s = 0.1$; (b) $\phi_s = 0.3$; (c) $\phi_s = 0.4$; (d) $\phi_s = 0.45$; (e) $\phi_s = 0.5$.

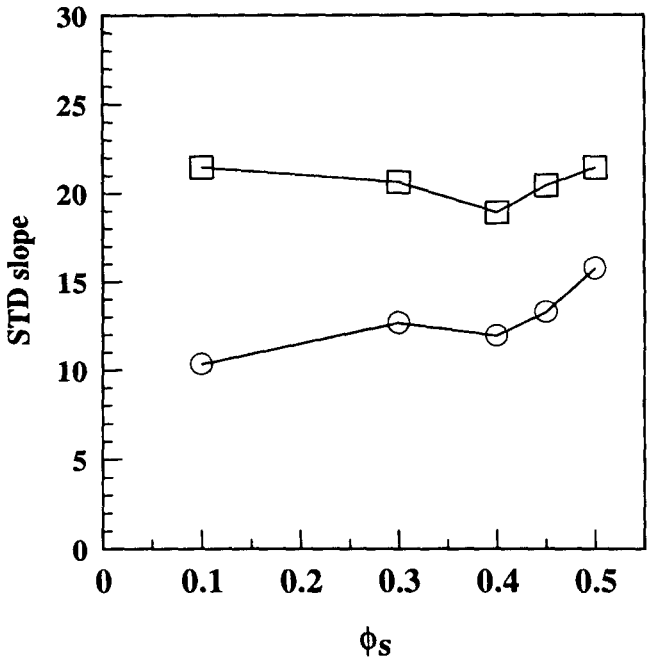

Figure 13. The dependence of the standard deviation slopes on the particle concentration. □, Vertical STD; ○, horizontal STD.

suspension. Furthermore, it should be remembered that our LDA technique is not yet capable of detecting whether the measured tracer is in the fluid, the solid particle or at the interface. Thus the accumulated data reflect primarily a periodic motion (rotation) while its average denote the net drift. The magnitude of the STD depends linearly on the magnitude of w_{max} as is evident in figures 12(a)–(e). Clearly, since the vorticity is proportional to w_{max}, the width of the flow cell is $2b$ and the particle radius is a, one should expect rotation velocities of $O(w_{max}a/b)$ which are similar in magnitude to the observed STD values. The intersections of the curves with the ordinates in figure 12 can be interpreted as noise not directly associated with the flow. It should be noted that it is significantly smaller than the STD and the magnitude of the vertical average velocities.

It is important to note that the STD normalized by w_{max} of each run, i.e. the part of the STD which is relative to the shear rate was found almost independent of the particle concentration as is evident in figure 13 where the slopes of the lines of figure 12 are depicted. This, again, strengthens the conclusion that the velocity fluctuations are primarily due to the local rotation velocities in the suspension since the latter depend linearly on the local shear rate, for a given w_{max}, which is the same for all suspension concentrations. Finally, one should note that the vertical STD are always greater than the horizontal STD. This may be due to the fact that particles which rotate in the x direction do not contribute rotation velocities to the horizontal component measurements. Only particles with a component of the rotation in the y direction do contribute. On the other hand, all rotating particles contribute to the vertical velocity STD. Thus, while the magnitude of the contribution is similar, the vertical STD is always larger.

4. CONCLUDING REMARKS

The on line technique of matching the refractive indices of the suspending fluid and the suspended particles facilitated the use of laser light in the bulk of the highly concentrated suspensions. It was shown that the relative intensity of the light signal has a clear exponential dependence on the refractive indices difference and on the particle concentration.

We have demonstrated the ability to use the laser light intensity to measure particle concentration in a flowing concentrated suspension. The transparency of the system made it possible to obtain

good laser Doppler signals in the bulk of the flow and to detect velocities down to 20 μm/s in suspensions with particle concentrations up to $\phi_s = 0.5$.

The method was applied successfully to obtain the longitudinal velocity profile of a viscous suspension flowing in a rectangular flow cell and the lateral velocity which stems from particle drift that exists in a flowing concentrated suspension and depends on the shear intensity. A detailed description of the hydrodynamics results is given in Part II.

Acknowledgements—This research was supported by the Basic Research Foundation administered by the Israel Academy of Sciences. Alexander Averbakh acknowledges support in part by the Israeli Ministry of Absorption.

REFERENCES

Abbas, M. A. and Crowe, C. T. (1987) Experimental study of the flow properties of a homogeneous slurry near transitional Reynolds numbers. *Int. J. Multiphase Flow* **13,** 357–364.

Abbott, J., Mondy, L. A., Graham, A. L. and Brenner, H. (1993) Techniques for analyzing the behavior of concentrated suspensions. In *Particular Two-phase Flow*, ed. M. C. Roco, Chapter 1. Butterworth-Heinemann, Boston.

Shauly, A., Averbakh, A., Nir, A. and Semiat, R. (1997) Slow viscous flows of highly concentrated suspensions—Part II: particle, migration velocity and concentration profiles in rectangular ducts. *Int. J. Multiphase Flow* **23.**

Drain, L. E. (1980) *The Laser–Doppler Technique*. Wiley, New York.

Durst, F., Melling, A. and Whitelaw, J. H. (1976) *Principles and Practice of Laser–Doppler Anemometry*. Academic Press, London.

Falco, R. and Nocera, D. (1993) Quantitative multipoint measurements and visualization of dense liquid–solid flows using laser induced photochemical anemometry (LIPA). In *Particulate Two-phase Flow*, ed. M. C. Roco, Chapter 3. Butterworth-Heinemann, Boston.

Ham, J. M. and Homsy, G. M. (1988) Hindered settling and hydrodynamic dispersion in quiescent sedimenting suspensions. *Int. J. Multiphase Flow* **14,** 533–546.

van de Hulst, H. C. (1957) *Light Scattering by Small Particles*. Wiley, New York.

Ioffe, B. V. (1974) *Refractometricheskie Metody Chimiy*. Chimia, Leningrad.

Ishimaru, A. (1978) *Wave Propagation and Scattering in Random Media*, Vol. 1. Academic Press, New York.

Koh, C. J., Hookham, P. and Leal, L. G. (1994) An experimental investigation of concentrated suspension flows in a rectangular channel. *J. Fluid Mech.* **266,** 1–32.

Kriger, I. M. (1972) Rheology of monodisperse latices. *Adv. Colloid Interface Sci.* **3,** 111–136.

Leighton, D. and Acrivos, A. (1987a) The shear induced migration of particles in concentrated suspensions. *J. Fluid Mech.* **181,** 415–439.

Leighton, D. and Acrivos, A. (1987b) Measurement of shear-induced self-diffusion in concentrated suspensions of spheres. *J. Fluid Mech.* **177,** 109–131.

Milliken, W. J., Gottlieb, M., Graham, L. A., Mondy, L. A. and Powell, R. L. (1989) The effect of the diameter of the falling ball on the apparent viscosity of suspensions of spheres and rods. *J. Fluid Mech.* **202,** 217–232.

Nouri, J. M., Whitelaw, J. H. and Yianneskis, M. (1986) An investigation of refractive index matching of continuous and discontinuous phases. *3rd Int. Symp. on Applications of Laser Anemometry to Fluid Mechanics*, Lisbon, Portugal.

Nouri, J. M., Whitelaw, J. H. and Yianneskis, M. (1988) Particle motion and turbulence in dense two-phase flows. *Int. J. of Multiphase Flow* **13,** 729–739.

Park, J. T., Manheimer, R. J., Grimley, T. A. and Morrow, T. B. (1989a) Velocity measurements of transparent non-Newtonian pipeline slurries with laser–Doppler anemometry. *Applications of Laser Anemometry to Fluid Mechanics*, eds R. J. Adrian, T. Asanuma, D. F. G. Durao and J. H. Whitelaw, pp. 292–312. Springer, Berlin.

Park, J. T., Manheimer, R. J., Grimley, T. A. and Morrow, T. B. (1989b) Pipe flow measurements of transparent non-Newtonian pipeline slurry. *J. Fluids Engng* **111,** 331.

Park. J. T., Grimley, T. A. and Manheimer, R. J. (1992) Turbulent velocity profile LDA measurements in pipe flow of non-Newtonian slurry with a yield stress. *6th Int. Symp. on Applications of Laser Techniques to Fluid Mechanics*. Lisbon, Portugal.

Philips, R. J., Armstrong, R. C., Brown, R. A., Graham, A. L. and Abbott, J. R. (1992) A constitutive equation for concentrated suspensions that accounts for shear-induced particle migration. *Phys. Fluids A* **4,** 30–40.

Schlichting, H. (1965) *Boundary Layer Theory*, 6th Edition. McGraw-Hill, New York.

Semiat, R. and Dukler, A. E. (1981) Simultaneous measurement of size and velocity of bubbles or drops—a new optical technique. *AiChE J.* **27,** 148–159.

Zisselmar, R. and Molerus, O. (1979) Investigation of solid–liquid pipe flow with regard to turbulent modification. *The Chemical Engineering Journal* **18,** 233–239.